

A magnetocaloric study on the series of 3d-metal chromites ACr_2O_4 where $\text{A} = \text{Mn}, \text{Fe}, \text{Co}, \text{Ni}, \text{Cu}$ and Zn

Anzar Ali^{1,*} and Yogesh Singh¹

¹*Department of Physical Sciences, Indian Institute of Science Education and Research,
Knowledge city, Sector 81, SAS Nagar, Manauli PO 140306, Mohali, Punjab, India*

The 3d-metal chromites ACr_2O_4 where A is magnetic ion, show the paramagnetic to ferrimagnetic phase transition at T_C while for non magnetic A-site ion, ACr_2O_4 show paramagnetic to antiferromagnetic phase transition at T_N . In this report, we present the detailed study of magnetic and the magnetocaloric effect (MCE) of the 3d-metal chromites ACr_2O_4 (where $\text{A} = \text{Mn}, \text{Fe}, \text{Co}, \text{Ni}, \text{Cu}$ and Zn) near T_C and T_N . We find the magnitude of MCE ($-\Delta S_M$) decreases on decreasing the magnetic moment of A-site ion with a exception for CuCr_2O_4 . Additionally, to know more about the order and nature of phase transition, we have made a scaling analysis of ($-\Delta S_M$) for all the chromites across the phase transition temperatures T_C and T_N .

I. INTRODUCTION

Spinel compounds with general formula AB_2O_4 ¹, where A-site is occupied by divalent cations and the B-site is occupied with trivalent cations, have attracted much attention in recent years due to their large magnetocapacitance^{2,3}, colossal magnetoresistance³⁻⁵ and tunable magnetocaloric effect⁶⁻⁸. In spinel chromites ACr_2O_4 ($A = 3d$ transitional metals, Mn, Fe, Co, Ni, Cu and Zn), the spin, orbital, and lattice degree of freedom play an essential role in the enhancement of multifunctional behavior such as magnetoelastic^{9,10}, magnetodielectric¹¹, multiferroic¹²⁻¹⁶ and magnetocaloric effect⁶. A deeper understanding of the interactions between spin, lattice, and orbital may provide a great way to use these spinels chromites with their fullest application potential.

The spinel chromites ACr_2O_4 where A-site is non-magnetic (Zn, Mg, Cd) show a high degree of frustration¹⁷. In such compounds, the antiferromagnetic nearest neighbor interaction between Cr^{3+} ions do not order to the lowest measured temperatures¹⁸. The spinel chromites where A-site is a magnetic 3d-transition metal ion show a ferrimagnetic ordering on cooling below some specific temperatures. The coupling between spin, lattice, and orbital degree of freedom leads to several magnetostructural transitions. All the spinels chromites ACr_2O_4 where A-site is Mn, Fe, Co, Ni, and Cu go through the ferrimagnetic ordering at the temperature $T_C = 41$ ¹⁹, 101 ²⁰, 97 ²¹, 68 ²², and $129K$ ²³ respectively, while $ZnCr_2O_4$ order antiferromagnetically at $T_N = 13K$ ²⁴. The coupled magnetostructural transitions have been observed and studied well for the chromites such as $MnCr_2O_4$ ¹¹, $FeCr_2O_4$ ²⁵, $CoCr_2O_4$ ¹¹, and $NiCr_2O_4$ ²⁶. In such spinels chromites with magnetic A-site, the structural changes occur at the ferrimagnetic ordering where system goes from tetragonal to orthorhombic symmetry^{27,28}. In general, the magnetostructural transitions are of first order in nature. In first order transitions, the order parameter changes abruptly and hence a massive change in the entropy of a system at the transition point is expected.

Generally, the rare-earth-based compounds have a large effective magnetic moment and show a giant magnetocaloric effect²⁹⁻³¹. A lot of experimental, theoretical work has been carried out to understand the magnetocaloric behavior of rare-earth-based materials^{32,33}. The rare-earth-based materials are expensive and get sometimes get oxidized in air. So it is customary to search materials which cost less and have higher stability in air. Recently, the transition metal oxide compounds have attracted much attention due to their interesting multifunctional behavior such as multiferroic and magnetocaloric effect. These interesting physical properties are due to an interplay among different degrees of freedom, such as spin, lattice, and orbital. The study of MCE on the series of spinel chromites may give some indications to understand and control such multifunctional behavior.

The work we are presenting in this report includes the comprehensive study of the magnetocaloric effect in the vicinity of the ferrimagnetic phase transition for ACr_2O_4 ($A = Mn, Fe, Co, Ni, \text{ and } Cu$) and across the antiferromagnetic transition for $ZnCr_2O_4$. We also include MCE results on $NiCr_2O_4$ from the previous reported work⁸ to be able to make a comparison. Additionally we have also made a entropy scaling analysis across these transitions to get insight into the governing mechanism and order of the magnetic phase transition.

II. EXPERIMENTAL DETAILS

The polycrystalline samples of spinels ACr_2O_4 where $A = Mn, Fe, Co, Ni, Cu$ and Zn have been synthesized using solid state reaction method. The starting materials AO (99:995%, Alfa Aesar) and Cr_2O_3 (99:999%, Alfa Aesar) were taken in the stoichiometry ratio. The reactants were mixed thoroughly and then pelletized using 5-ton pressure. All the pelletized materials then placed in alumina crucibles covered with a lid except $MnCr_2O_4$ and $FeCr_2O_4$. The pelletized mixture of $MnCr_2O_4$ and $FeCr_2O_4$ were sealed in the evacuated quartz tube and then loaded into box furnace. Several heat treatments with intermediate grindings were given with temperatures as mentioned in the Table I.

Room temperature powder X-ray diffraction of all spinels ACr_2O_4 where $A = Mn, Fe, Co, Ni, Cu$ and Zn compounds are refined by Rietveld refinement method using GSAS software. The spinels $MnCr_2O_4$, $FeCr_2O_4$, $CoCr_2O_4$, and $ZnCr_2O_4$ crystallize in cubic group $Fd\bar{3}m$ while $NiCr_2O_4$ and $CuCr_2O_4$, which contain Jahn-Teller active Ni^{2+} and Cu^{2+} ions crystallize in tetragonal space group $I4_1/amd$. The refined lattice parameters are listed in Table (II) and match well with the literature^{7,23,25,26,34}. The magnetic measurements were performed using Quantum Design (QD) physical property measurement system (PPMS).

III. RESULT AND DISCUSSION

Figure 1 shows magnetization versus temperature, $M(T)$, measured under zero-field cooled (ZFC) and field cooled (FC) protocol in an applied field of 0.1T. The sharp increase of magnetization at temperature $T_C = 41, 101, 97, 68, \text{ and } 129K$ in $MnCr_2O_4$, $FeCr_2O_4$, $CoCr_2O_4$, $NiCr_2O_4$, and $CuCr_2O_4$ respectively indicate the ferromagnetic or

ferrimagnetic ordering. These transitions are well studied in literature and identified as ferrimagnetic ordering between A^{2+} and Cr^{3+} . $ZnCr_2O_4$ order antiferromagnetically at $T_N = 13K$.

Figure 2 shows magnetization versus field, $M(H)$ measured at various temperatures indicated in the plots for all the spinels $MnCr_2O_4$, $FeCr_2O_4$, $CoCr_2O_4$, $NiCr_2O_4$, $CuCr_2O_4$, and $ZnCr_2O_4$ compounds. All the spinels shows the characteristic of soft ferrimagnet with a tendency for rapid saturation accompanied by a small coercivity except $ZnCr_2O_4$, which shows a linear field dependent magnetization, which is typical behavior for an antiferromagnetic phase. In these spinels $FeCr_2O_4$ shows highest coercivity and $MnCr_2O_4$ shows minimum coercivity. The $M(H)$ however, never saturates even at our highest applied magnetic fields suggesting that there is a paramagnetic or antiferromagnetic component at all measured temperatures. This suggests that some magnetic ions do not participate in ferrimagnetic ordering.

To understand field dependent magnetic behavior of these samples over a broad temperature range and to calculate its magnetocaloric potential, $M(T, H)$ is obtained from measurement of M vs H at various temperatures. Figure 3 shows the series of isotherms $M(T, H)$ measured for all the spinel compounds in the temperature and field ranges indicated in the plots. $M(T, H)$ isotherms were measured at different temperature with 2 K interval. When an external magnetic field is applied to a magnetic material, its atom's magnetic moment try to align along the applied magnetic field and hence its magnetic entropy decreases. Under adiabatic process, the temperature of the material increases. Conversely when applied magnetic field is removed adiabatically, the temperature of material decreases. This thermal response of magnetic material in the varying magnetic field is called magnetocaloric effect (MCE). The magnetocaloric effect is related to the change in magnetic entropy $-\Delta S_M$ and it can be calculated by applying Maxwell's thermodynamic relation as stated below⁶:

$$\Delta S_M(T, H_{0 \rightarrow H_{MAX}}) = \mu_0 \int_0^{H_{MAX}} \left| \frac{dM}{dT} \right|_H dH \quad (1)$$

Another important parameter of a MCE material is the cooling efficiency also called relative cooling power (RCP)³⁵. RCP is defined by the expression:

$$RCP = -\Delta S_M(T, H) \times \Delta T_{FWHM} \quad (2)$$

The temperature dependence of $-\Delta S_M$ vs T thus obtained from a series of isothermal magnetization at various temperature for all the spinels across the magnetic transition at T_C and T_N are shown in figure 4. The magnitude of the peak of $-\Delta S_M$ increases with increasing magnetic field as expected. The temperature range for significant magnetocaloric effect can be estimated from the full width at half maximum (FWHM) of $-\Delta S_M$. The values of maximum entropy change $-\Delta S_M$, ΔT_{FWHM} , RCP and transition temperature (T_C) have been calculated for all the spinel samples. All the ACr_2O_4 where A is magnetic ion show the positive value of maximum entropy change ($-\Delta S_M$) while $ZnCr_2O_4$ has negative value of maximum entropy change ($-\Delta S_M$) which is expected across AFM-PM transition. The magnetocaloric parameters for all the ACr_2O_4 where A = Mn, Fe, Co, Ni, Cu and Zn compounds in a external magnetic field of strength 9T, together with some other spinels materials are listed in the Table III for comparison. The maximum entropy change ($-\Delta S_M$) and RCP increase with the increase of A-site spin magnetic moment and we get highest $-\Delta S_M$ and RCP for $MnCr_2O_4$. This behavior suggest that the degree of magnetization in these spinels near paramagnetic to ferrimagnetic phase transition is highly coupled with the A-site magnetic moment. However, this trend deviate for the spinel $CuCr_2O_4$. To find the origin of this deviation further microscopic investigation are needed.

In order to get insight about the nature of the magnetic transition in the vicinity of the transition temperature we have done scaling analysis of the maximum entropy change. According to mean field model the magnetic entropy change at the transition is expected to follow a power law behavior given by $-\Delta S_M \propto H^n$ with $n = 2/3$ ³⁶. Figure 5 shows the plot of ΔS_M versus $H^{2/3}$ for the magnetic transition at T_0 for all the spinels $MnCr_2O_4$, $FeCr_2O_4$, $CoCr_2O_4$, $NiCr_2O_4$, $CuCr_2O_4$, and $ZnCr_2O_4$ compounds. $FeCr_2O_4$, $CoCr_2O_4$, and $NiCr_2O_4$ show a nearly linear plot, which strongly suggests that these transition are mean-field like. The plots ΔS_M versus $H^{2/3}$ for $MnCr_2O_4$, $CuCr_2O_4$, and $ZnCr_2O_4$ deviate from linearity, indicating non mean field like transitions in these compounds.

Franco *et al.*³⁷ gave a model for the materials which has second order magnetic phase transition. They proposed that the $\Delta S_M(T)$ curves at different magnetic fields are expected to collapse onto a common universal curve when they are plotted as $\Delta S_M / \Delta S_M^{max}$ versus θ , where ΔS_M^{max} is the value of ΔS_M at the transition temperature around which the scaling analysis is being made, and θ is a reduced temperature given by $\theta = -\frac{T-T_c}{T_{r1}-T_c}$ for $T \leq T_c$ and $\theta = \frac{T-T_c}{T_{r2}-T_c}$ for $T > T_c$. The T_{r1} and T_{r2} are the temperatures at the full width at half maximum of the anomaly in ΔS_M . We have performed the above scaling analysis for all the spinels $MnCr_2O_4$, $FeCr_2O_4$, $CoCr_2O_4$, $NiCr_2O_4$, $CuCr_2O_4$, and $ZnCr_2O_4$ compounds.

The plot of $\Delta S_M / \Delta S_M^{max}$ at various fields versus the reduced parameter θ is shown in Fig. 6 for all the compounds. We see that all the ΔS_M curves for the different magnetic fields approximately collapse onto a single universal master curve except for ZnCr_2O_4 . This is strong evidence of the second order nature of the magnetic transition at T_C in spinels MnCr_2O_4 , FeCr_2O_4 , CoCr_2O_4 , NiCr_2O_4 , and CuCr_2O_4 compounds while the magnetic transition in ZnCr_2O_4 is of first order.

IV. CONCLUSIONS

In this work we study the magnetocaloric (MCE) response ($-\Delta S_M$) of all the spinels MnCr_2O_4 , FeCr_2O_4 , CoCr_2O_4 , NiCr_2O_4 , CuCr_2O_4 , and ZnCr_2O_4 compounds across their magnetic transition T_C and T_N . The spinels ACr_2O_4 where A^{2+} is a magnetic ion show paramagnetic to ferrimagnetic phase transition at temperature T_C . The spinels ACr_2O_4 where A^{2+} is non-magnetic ion show paramagnetic to antiferromagnetic phase transition at temperature T_N . We observed that MnCr_2O_4 shows a maximum value of MCE in all the studied here spinel chromites while ZnCr_2O_4 shows inverse MCE. It is clear to say that the degree of MCE ($-\Delta S_M^{max}$) depends on the magnetic moment of A-site ion in ACr_2O_4 . The MCE ($-\Delta S_M^{max}$) of the spinels decrease on decrease of A-site spin magnetic moment for all the spinels except for CuCr_2O_4 . Further microscopic probe studies will be required to clarify the origin of this exception for CuCr_2O_4 .

V. ACKNOWLEDGMENT

We acknowledge the support of the X-ray facility at IISER Mohali for powder XRD measurements.

Table I. Synthesis temperature conditions for ACr_2O_4 .

ACr_2O_4	Heat Treatments			Environment
	First	Second	Third	
NiCr_2O_4	800°/24h	1100°/24h	110°/24h	in air
CoCr_2O_4	800°/24h	1000°/24h	1000°/24h	in air
CuCr_2O_4	1100°/24h	1200°/24h	1200°/24h	in air
ZnCr_2O_4	800°/24h	1200°/24h	1200°/24h	in air
MnCr_2O_4	1100°/24h	1200°/24h	1300°/24h	in inert
FeCr_2O_4	800°/24h	1000°/24h	13000°/24h	in inert

Table II. Space group and refined lattice parameters of ACr_2O_4 for the powder X-ray diffraction data taken at room temperature.

ACr_2O_4	Space group	a (Å)	b (Å)	c (Å)	$\alpha = \beta = \gamma$
MnCr_2O_4	$\text{Fd}\bar{3}\text{m}$	8.4374(1)	8.4374(1)	8.4374(1)	90°
FeCr_2O_4	$\text{Fd}\bar{3}\text{m}$	8.3922(1)	8.3922(1)	8.3922(1)	90°
CoCr_2O_4	$\text{Fd}\bar{3}\text{m}$	8.3364(1)	8.3364(1)	8.3364(1)	90°
NiCr_2O_4	$\text{I}4_1/\text{amd}$	5.8763(1)	5.8763(1)	8.3180(2)	90°
CuCr_2O_4	$\text{I}4_1/\text{amd}$	6.0327(2)	6.0327(2)	7.7958(3)	90°
ZnCr_2O_4	$\text{Fd}\bar{3}\text{m}$	8.3284(1)	8.3284(1)	8.3284(1)	90°

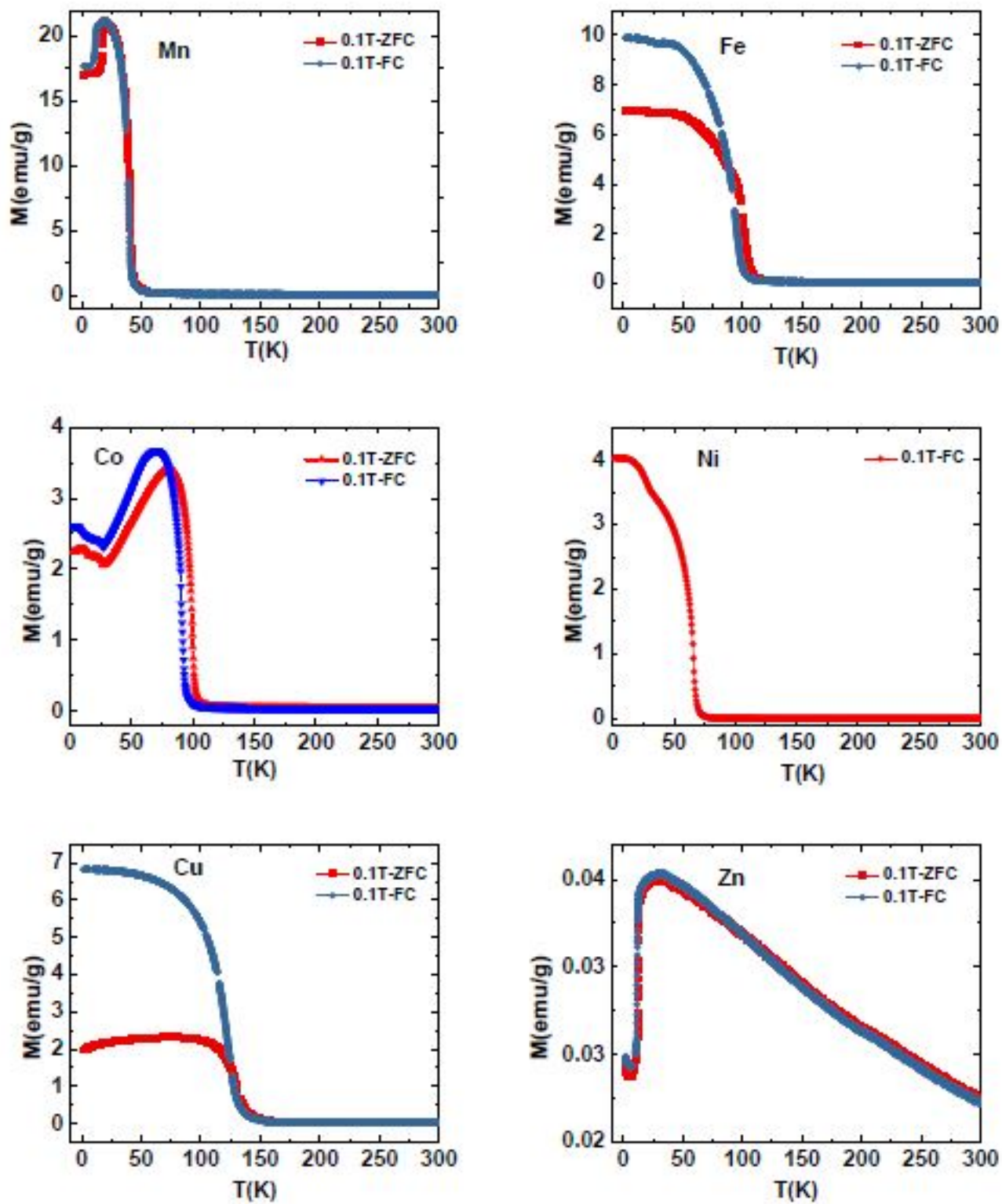


Figure 1. ZFC and FC magnetization curves recorded under magnetic field $H = 0.1$ T for all the compounds indicated in the plots.

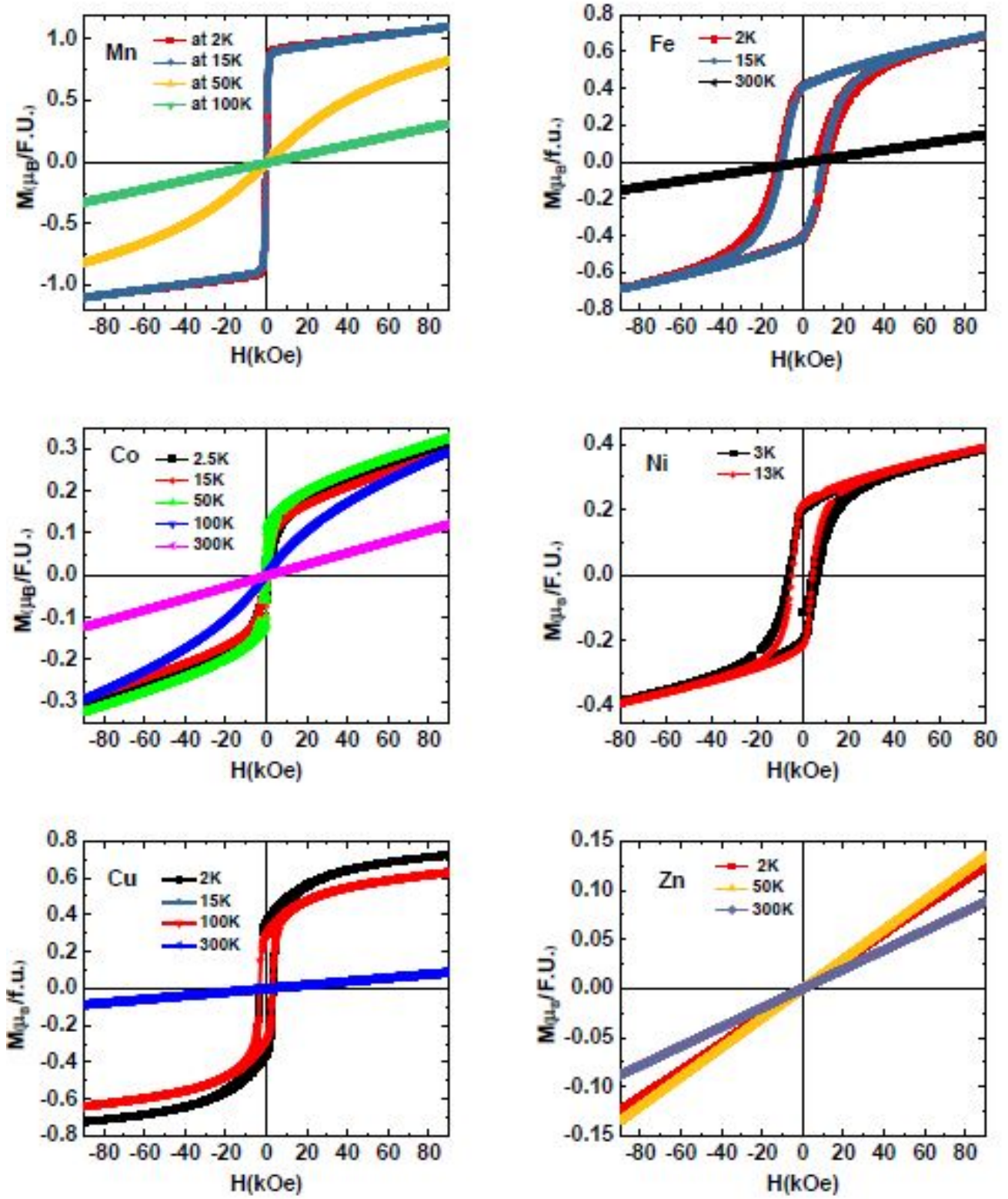


Figure 2. Isothermal curves of magnetization verses magnetic field for all the ACr_2O_4 where $A = \text{Mn, Fe, Co, Ni, Cu}$ and Zn compounds at various temperatures indicated in the plots.

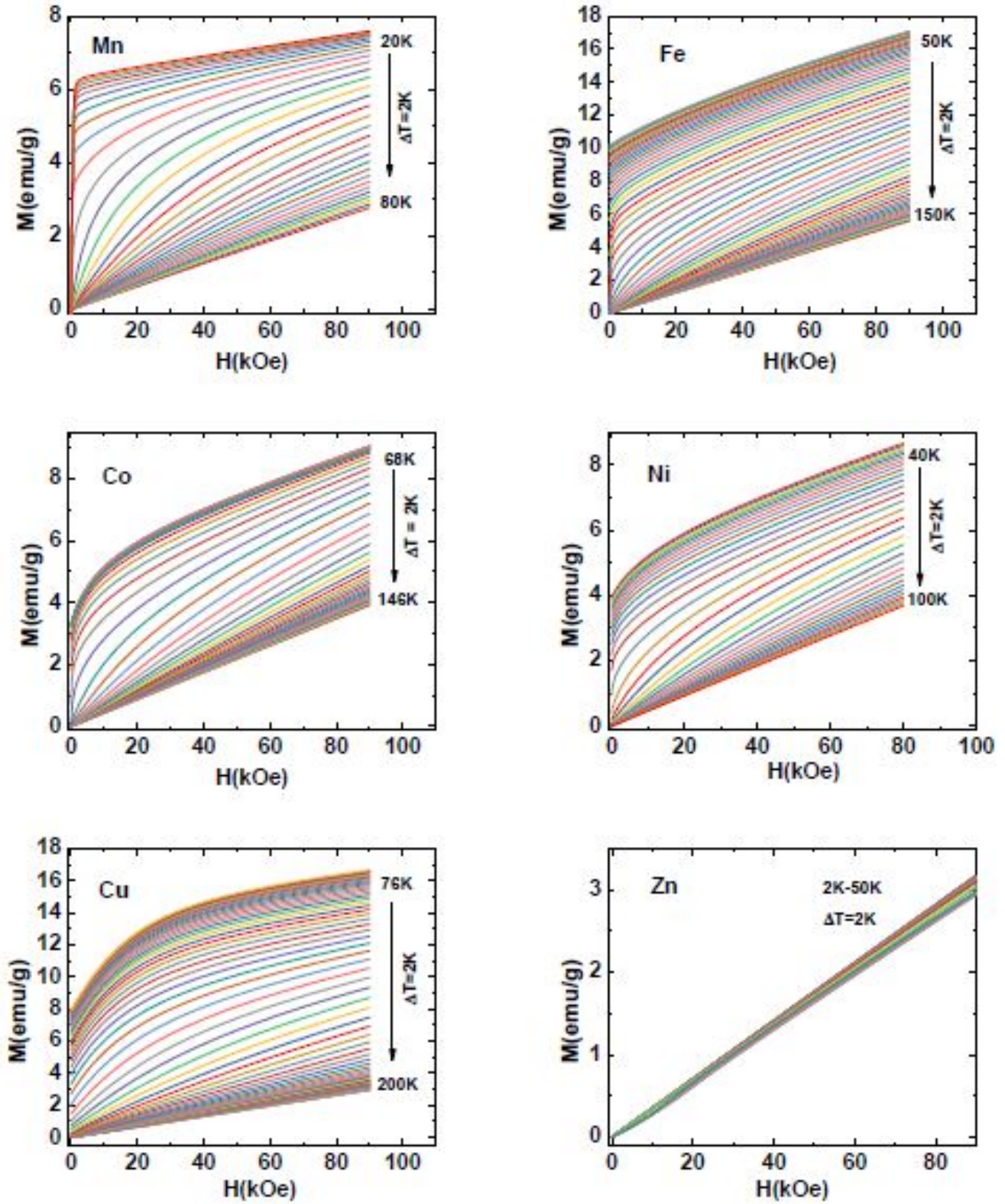


Figure 3. Series of isotherms of magnetization with a step size of $\Delta T = 2K$ for ACr_2O_4 where $A = Mn, Fe, Co, Ni, Cu$ and Zn compounds in the temperature ranges indicated in the plots.

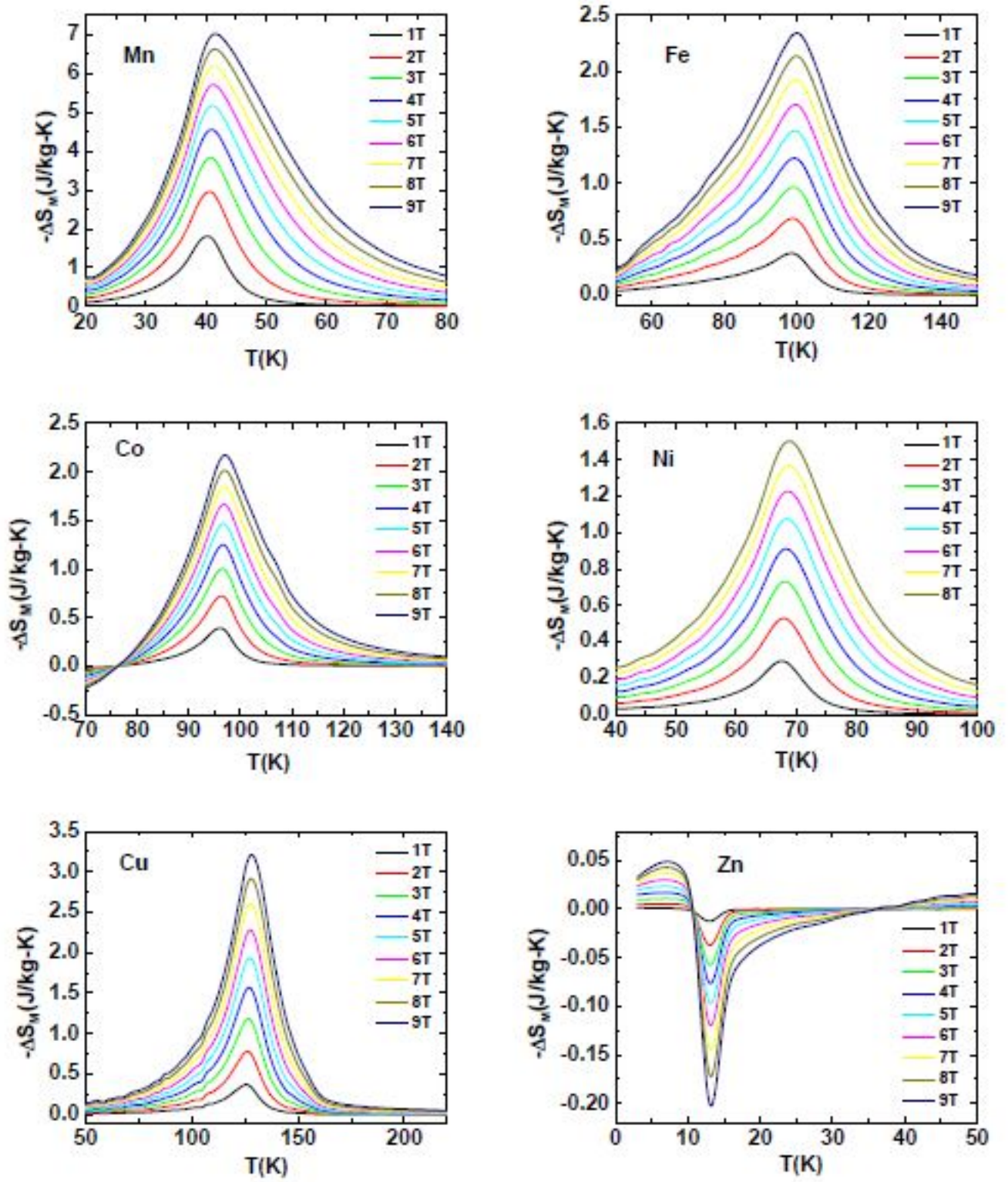


Figure 4. The thermal profile of field induced change in magnetic entropy, $-\Delta S_M$, calculated from Maxwell's equation 1 using isothermal magnetization curves in the vicinity of transition temperature for all the ACr_2O_4 where $A = Mn, Fe, Co, Ni, Cu$ and Zn compounds at various external magnetic field as indicated in the plots.

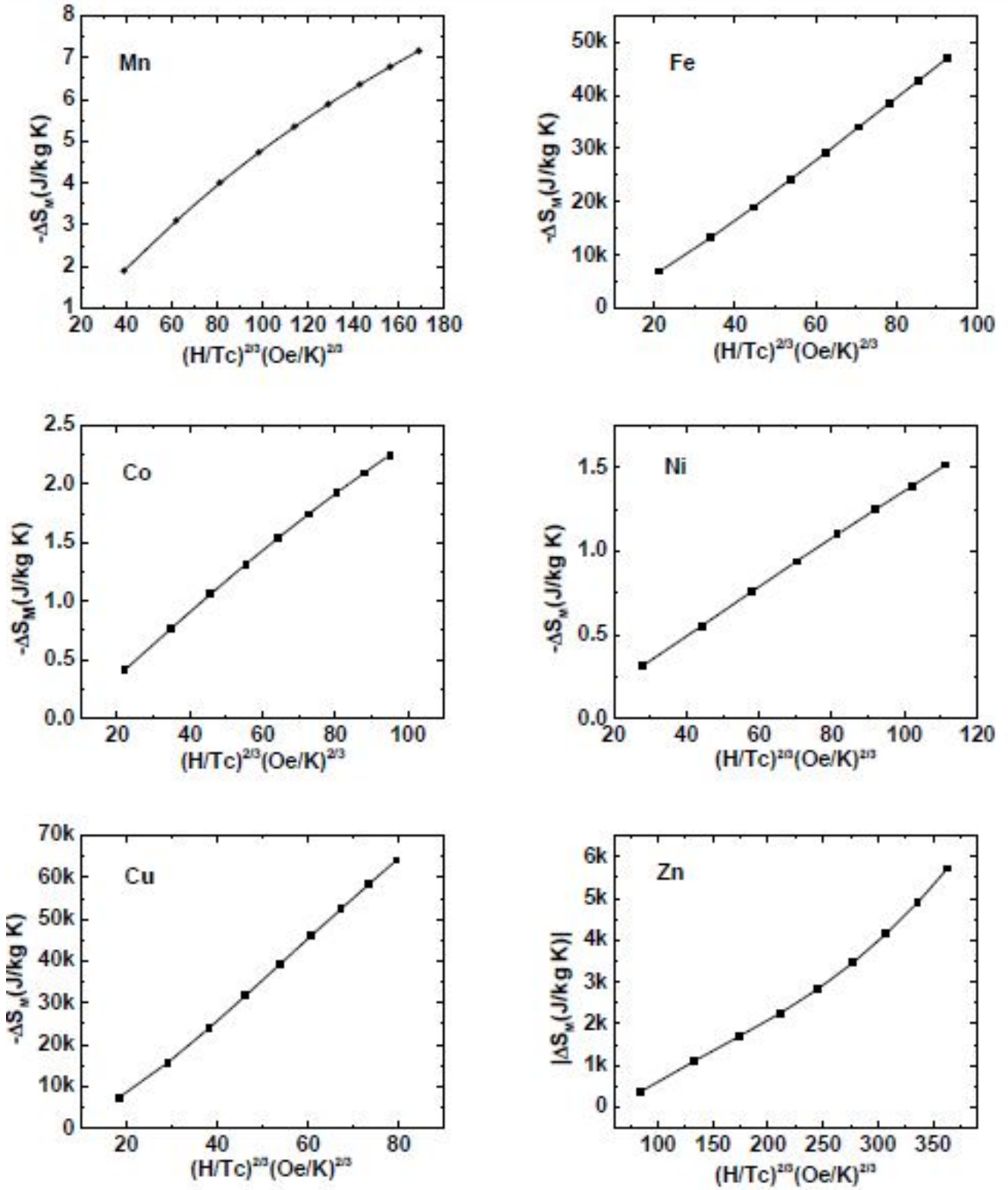


Figure 5. ΔS_M^{max} versus $H^{2/3}$ data showing a linear dependence expected for a mean-field transition.

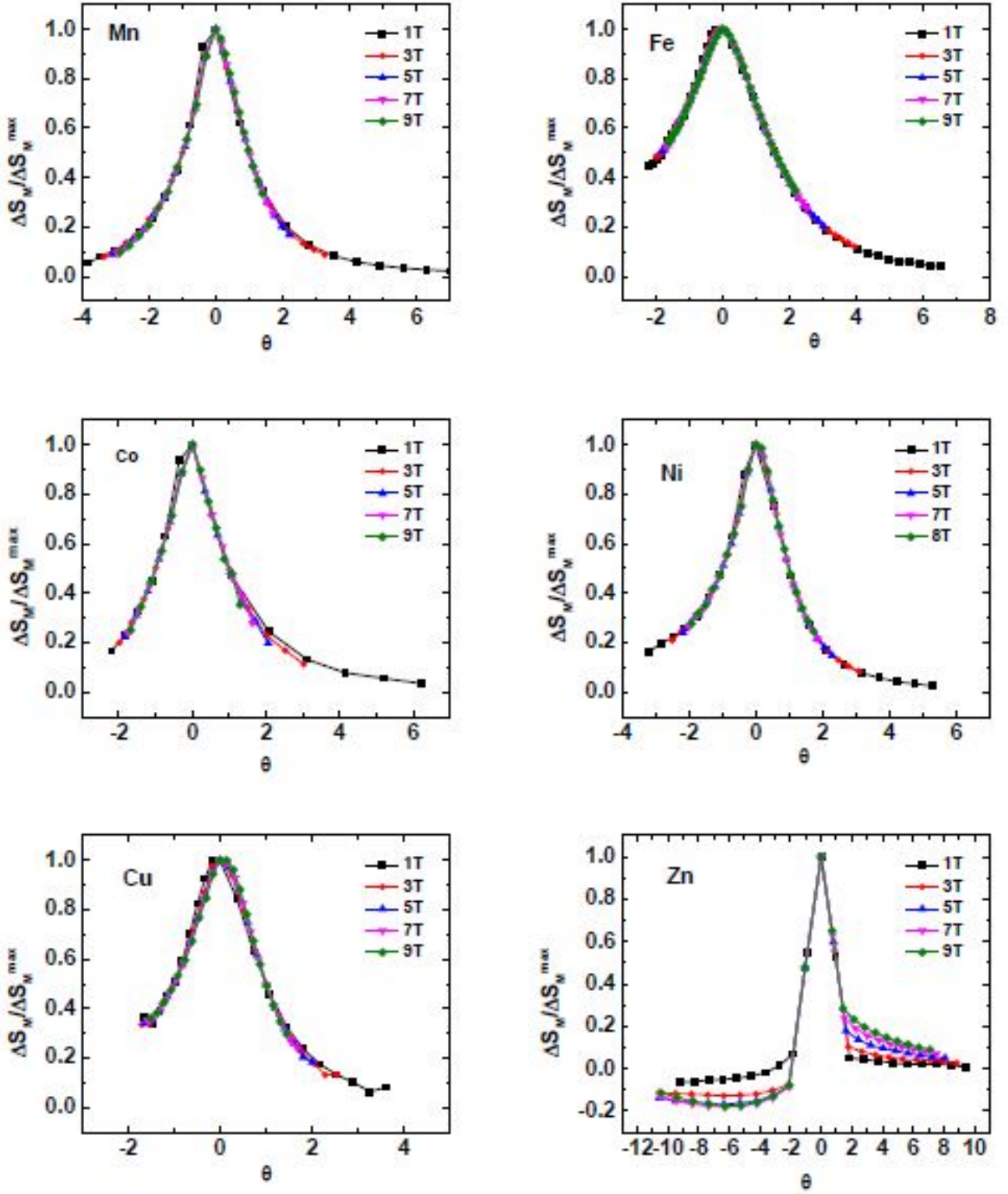


Figure 6. The collapse of all the ΔS_M data at different magnetic fields onto a universal curve when plotted as $\Delta S_M / \Delta S_M^{\max}$ vs θ

Table III. Table for each A site ion the value of S, effective magnetic moment³⁸, magnetocaloric parameters and transition temperature for all the ACr₂O₄ where A = Mn, Fe, Co, Ni, Cu and Zn compounds in a external magnetic field of strength 9T).

ACr ₂ O ₄	S	M(μ_B)	$-\Delta S_M$ (J/kg-K)	ΔT_{FWHM} (K)	RCP (J/kg)	T _C or T _N (K)
MnCr ₂ O ₄	2.5	5.92	7.16	28	200.48	41
FeCr ₂ O ₄	2.0	4.90	2.35	28	65.8	101
CoCr ₂ O ₄	1.5	3.87	2.25	17	38.35	97
NiCr ₂ O ₄	1.0	2.83	1.5	25	37.5	68
CuCr ₂ O ₄	0.5	1.73	3.22	24	77.28	129
ZnCr ₂ O ₄	0.0	0.0	-0.2	2.34	0.468	13
CdCr ₂ S ₄ ³⁹	–	–	7.04 at 4T	–	–	87
MnV ₂ O ₄ ⁴⁰	–	–	24.0 at 4T	–	–	57
Cd _{0.8} Cu _{0.2} Cr ₂ S ₄ ⁴¹	–	–	5.1 at 5T	–	–	86

* anzarali@iisermohali.ac.in

- ¹ W. H. BRAGG, *Nature* **95**, 561 (1915).
- ² J. Hemberger, P. Lunkenheimer, R. Fichtl, H.-A. Krug von Nidda, V. Tsurkan, and A. Loidl, *Nature* **434**, 364 (2005).
- ³ S. Weber, P. Lunkenheimer, R. Fichtl, J. Hemberger, V. Tsurkan, and A. Loidl, *Phys. Rev. Lett.* **96**, 157202 (2006).
- ⁴ A. P. Ramirez, R. J. Cava, and J. Krajewski, *Nature* **386**, 156 (1997).
- ⁵ H. W. Lehmann and M. Robbins, *Journal of Applied Physics* **37**, 1389 (1966), <https://doi.org/10.1063/1.1708485>.
- ⁶ V. Franco, J. Blázquez, B. Ingale, and A. Conde, *Annual Review of Materials Research* **42**, 305 (2012), <https://doi.org/10.1146/annurev-matsci-062910-100356>.
- ⁷ K. Dey, A. Indra, S. Majumdar, and S. Giri, *Journal of Magnetism and Magnetic Materials* **435**, 15 (2017).
- ⁸ A. Ali, G. Sharma, and Y. Singh, arXiv e-prints, arXiv:1811.07836 (2018), [arXiv:1811.07836 \[cond-mat.str-el\]](https://arxiv.org/abs/1811.07836).
- ⁹ S. Lee, A. Pirogov, M. Kang, K.-H. Jang, M. Yonemura, T. Kamiyama, S.-W. Cheong, F. Gozzo, N. Shin, H. Kimura, Y. Noda, and J.-G. Park, *Nature* **451**, 805 EP (2008).
- ¹⁰ M. Lapine, I. V. Shadrivov, D. A. Powell, and Y. S. Kivshar, *Nature Materials* **11**, 30 EP (2011).
- ¹¹ N. Mufti, A. A. Nugroho, G. R. Blake, and T. T. M. Palstra, *Journal of Physics: Condensed Matter* **22**, 075902 (2010).
- ¹² W. Eerenstein, N. D. Mathur, and J. F. Scott, *Nature* **442**, 759 (2006).
- ¹³ M. Bibes and A. Barthélémy, *Nature Materials* **7**, 425 EP (2008).
- ¹⁴ S.-W. Cheong and M. Mostovoy, *Nature Materials* **6**, 13 EP (2007), review Article.
- ¹⁵ R. Ramesh and N. A. Spaldin, *Nature Materials* **6**, 21 EP (2007), review Article.
- ¹⁶ M. Fiebig, T. Lottermoser, D. Meier, and M. Trassin, *Nature Reviews Materials* **1**, 16046 EP (2016), review Article.
- ¹⁷ R. Moessner and J. T. Chalker, *Phys. Rev. Lett.* **80**, 2929 (1998).
- ¹⁸ G.-W. Chern, R. Moessner, and O. Tchernyshyov, *Phys. Rev. B* **78**, 144418 (2008).
- ¹⁹ K. Dey, S. Majumdar, and S. Giri, *Phys. Rev. B* **90**, 184424 (2014).
- ²⁰ A. Maignan, C. Martin, K. Singh, C. Simon, O. Lebedev, and S. Turner, *Journal of Solid State Chemistry* **195**, 41 (2012), polar Inorganic Materials: Design Strategies and Functional Properties.
- ²¹ K. Tomiyasu, J. Fukunaga, and H. Suzuki, *Phys. Rev. B* **70**, 214434 (2004).
- ²² K. Tomiyasu and I. Kagomiya, *Journal of the Physical Society of Japan* **73**, 2539 (2004), <https://doi.org/10.1143/JPSJ.73.2539>.
- ²³ T. T. Gurgel, M. A. Buzinaro, and N. O. Moreno, *Journal of Superconductivity and Novel Magnetism* **26**, 2557 (2013).
- ²⁴ Y. Jo, J.-G. Park, H. C. Kim, W. Ratcliff, and S.-W. Cheong, *Phys. Rev. B* **72**, 184421 (2005).

- ²⁵ K. Singh, A. Maignan, C. Simon, and C. Martin, *Applied Physics Letters* **99**, 172903 (2011), <https://doi.org/10.1063/1.3656711>.
- ²⁶ T. D. Sparks, M. C. Kemei, P. T. Barton, R. Seshadri, E.-D. Mun, and V. S. Zapf, *Phys. Rev. B* **89**, 024405 (2014).
- ²⁷ M. R. Suchomel, D. P. Shoemaker, L. Ribaud, M. C. Kemei, and R. Seshadri, *Phys. Rev. B* **86**, 054406 (2012).
- ²⁸ N. Stüsser, M. Reehuis, M. Tovar, B. Klemke, A. Hoser, and J.-U. Hoffmann, *Phys. Rev. B* **98**, 144424 (2018).
- ²⁹ V. K. Pecharsky and K. A. Gschneidner, Jr., *Phys. Rev. Lett.* **78**, 4494 (1997).
- ³⁰ I. G. de Oliveira, P. J. von Ranke, M. El Massalami, and C. M. Chaves, *Phys. Rev. B* **72**, 174420 (2005).
- ³¹ M. Wali, R. Skini, M. Khelifi, E. Dhahri, and E. K. Hlil, *Dalton Trans.* **44**, 12796 (2015).
- ³² B. G. Shen, J. R. Sun, F. X. Hu, H. W. Zhang, and Z. H. Cheng, *Advanced Materials* **21**, 4545 (2009), <https://onlinelibrary.wiley.com/doi/pdf/10.1002/adma.200901072>.
- ³³ A. Ali, G. Sharma, A. Vardhan, K. Pasrija, S. Rajput, T. Maitra, S. Kumar, and Y. Singh, *Journal of Physics: Condensed Matter* **31**, 305803 (2019).
- ³⁴ S.-H. Lee, C. Broholm, T. H. Kim, W. Ratchiff, and S.-W. Cheong, *Phys. Rev. Lett.* **84**, 3718 (2000).
- ³⁵ M. Wood and W. Potter, *Cryogenics* **25**, 667 (1985).
- ³⁶ H. Oesterreicher and F. T. Parker, *Journal of Applied Physics* **55**, 4334 (1984), <https://doi.org/10.1063/1.333046>.
- ³⁷ V. Franco and A. Conde, *International Journal of Refrigeration* **33**, 465 (2010).
- ³⁸ S. . Blundell, *Magnetism in condensed matter* (Oxford ; New York : Oxford University Press, 2001., 2001) includes bibliographical references and index.
- ³⁹ L. Q. Yan, J. Shen, Y. X. Li, F. W. Wang, Z. W. Jiang, F. X. Hu, J. R. Sun, and B. G. Shen, *Applied Physics Letters* **90**, 262502 (2007), <https://doi.org/10.1063/1.2751576>.
- ⁴⁰ X. Luo, Y. P. Sun, L. Hu, B. S. Wang, W. J. Lu, X. B. Zhu, Z. R. Yang, and W. H. Song, *Journal of Physics: Condensed Matter* **21**, 436010 (2009).
- ⁴¹ J. Shen, L.-Q. Yan, J. Zhang, F.-W. Wang, J.-R. Sun, F.-X. Hu, C.-B. Rong, and Y.-X. Li, *Journal of Applied Physics* **103**, 07B315 (2008), <https://doi.org/10.1063/1.2830973>.
- ⁴² V. Franco, J. S. Blázquez, and A. Conde, *Applied Physics Letters* **89**, 222512 (2006), <https://doi.org/10.1063/1.2399361>.
- ⁴³ V. Chaudhary, D. V. Maheswar Repaka, A. Chaturvedi, I. Sridhar, and R. V. Ramanujan, *Journal of Applied Physics* **116**, 163918 (2014), <https://doi.org/10.1063/1.4900736>.
- ⁴⁴ K. Tomiyasu, J. Fukunaga, and H. Suzuki, *Phys. Rev. B* **70**, 214434 (2004).
- ⁴⁵ A. Biswas, S. Chandra, T. Samanta, M. H. Phan, I. Das, and H. Srikanth, *Journal of Applied Physics* **113**, 17A902 (2013), <https://doi.org/10.1063/1.4793768>.